FINITE ELEMENT ANALYSIS OF CUTTING RESISTANCE IN FOUNDATION DESIGN

Zoltán CZAP

Hungarian Academy of Sciences
Research Group of Applied Mechanics
Department of Geotechnique Technical University of Budapest
H-1521 Budapest, Hungary
Tel/Fax: (+36 1) 166 4242

Received: March 25, 1994

Abstract

Cutting resistance values suggested by Jáky and Kézdi for determining load capacities of spread and deep footings have been compared to computer outputs. In conformity with analytic and numerical analysis results, FEM is suggested for compiling tables or diagrams for designing concrete strip and pier footings. The required material characteristics of concrete are defined and the possible procedure of computations outlined.

Keywords: finite element method, cutting resistance, PLAXIS, soil plasticity.

Introduction

In 1945, József JÁKY reported of his cutting resistance investigations (JÁKY, 1945). This subject was later dealt with by Árpád KÉZDI (1970). Compressive strength of cutter-shaped solids has been checked by the FEM program PLAXIS 4.5 (VERMEER, 1993) for the purpose of developing a design method for concrete foundations helped by diagrams. Reckoning with certain geometrical limitations, results showed a fair agreement, but beyond these limits, analytic results have become useless.

The concept of cutting resistance 'If the compressed solid has the form of a cutter with truncated top surface, c. e. with lateral surfaces other than horizontal but making an angle ϑ to the vertical, then the vertically loaded softer solid fails at a so-called cutting resistance p_v, a load less than the resistance (p_{sz}), i. e. the material glides away from the load along curved sliding surfaces' (*Fig. 1*).

Jáky's formula for the cutting resistance:

$$p_v = \sigma_{ny} \frac{1-\sin\varphi}{2\sin\varphi}\left[\tan^2\left(45^\circ + \frac{\varphi}{2}\right)e^{2\vartheta\tan\varphi} - 1\right], \qquad (1)$$

where:
p_v – cutting resistance according to *Fig. 1*;
σ_{ny} – unconfined compressive strength;
φ – angle of internal friction;
ϑ – half of the cutting angle according to *Fig. 1*.

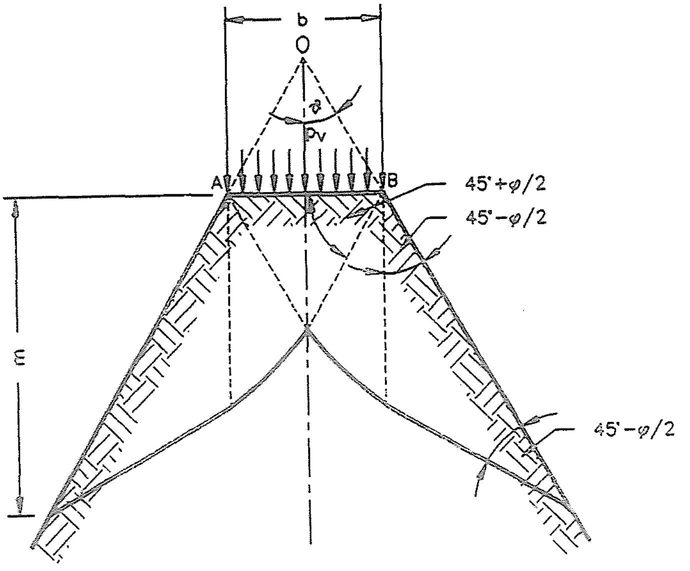

Fig. 1. The concept of cutting resistance

Elevation m required for undisturbed sliding:

$$m = be^{\vartheta \tan \varphi} \tan\left(45^\circ + \frac{\varphi}{2}\right) \cos\vartheta, \tag{2}$$

where b – width of cutter-shaped solid (*Fig. 1*).

The continuous lines in *Fig. 2* show the load bearing factor according to (1) (ratio of the cutting resistance to the unconfined compressive strength of the material) for various internal frictional angles (0°, 20°, 40°, 60°) and half cutting angles (0°, 15°, 30°, 45°, 60°) while *Fig. 3* shows the ratio of the height m of the soil failure pattern to the cutter width b. The cutting angles comprise the range of geometrical shapes of footings used in practice while internal friction values represent soils and concretes.

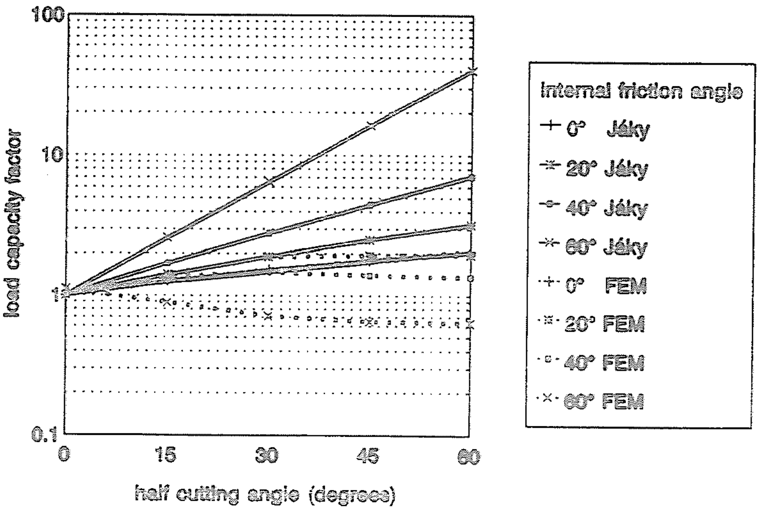

Fig. 2. Load capacity factors

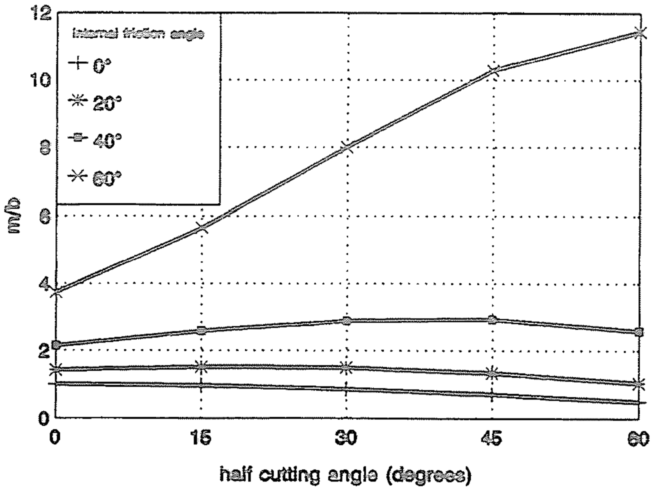

Fig. 3. Form factor of the failure pattern

Finite Element Analyses

In order to check load capacity according to (1), computations were made by the FEM program PLAXIS 4.5 (VERMEER, 1993). Computations were based on an elasto-plastic (Mohr–Coulomb) material model. Geometrical shape, boundary conditions and finite elements net for two typical cases are seen in *Fig. 4*. Triangles in the net are refined units, with further three nodal points each at their edges between vertices and three inside the elements so the displacement field within the units will be approximated by complete biquadratic polynomial. Load acts on the top face as seen in *Fig. 1*.

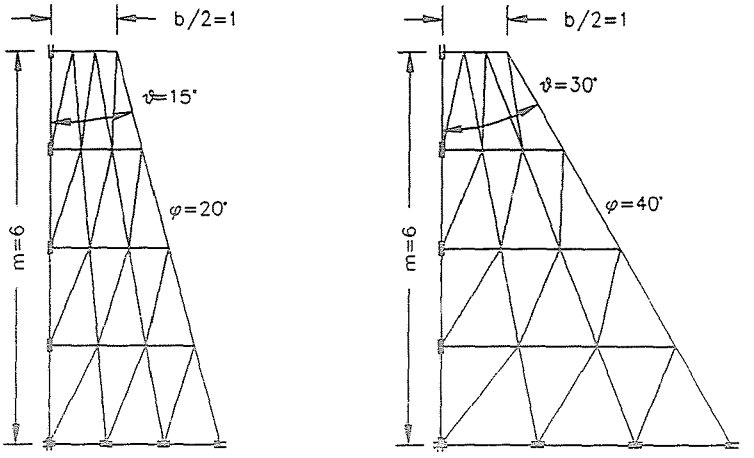

Fig. 4. Geometry and division of the finite element model

Further material characteristics applied in FEM:

$$\text{cohesion}, c = 100 \text{ kPa};$$
$$\text{shear modulus}, G = 100 \text{ MPa};$$

Poisson's ratio:

$$\mu = \frac{1 - \sin\varphi}{2 - \sin\varphi} \leq 0.495. \tag{3}$$

(In conformity with Jáky's formula for earth pressure at rest restriction is needed for stability of the numerical solution), unconfined compressive strength:

$$\sigma_{ny} = 2c \tan\left(45^\circ + \frac{\varphi}{2}\right). \tag{4}$$

Confrontation of Results

Load capacity factor obtained by the FEM (ratio of cutting resistance to unconfined compressive strength of the material) for the same internal friction angles and half cutting angles as those involved in the analytic test are seen in *Fig. 2.*

Significant differences between the results of analytic and numerical investigations (*Fig. 2*) are substantiated by the results shown in *Figs 5, 6* and *7.*

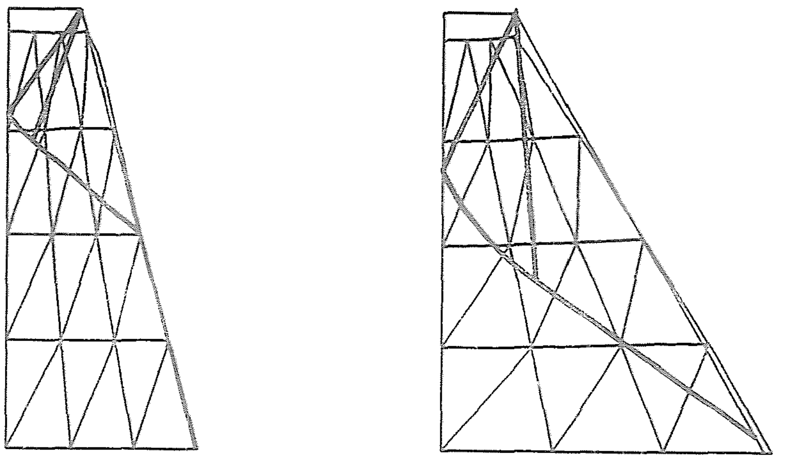

Fig. 5. Network deformation

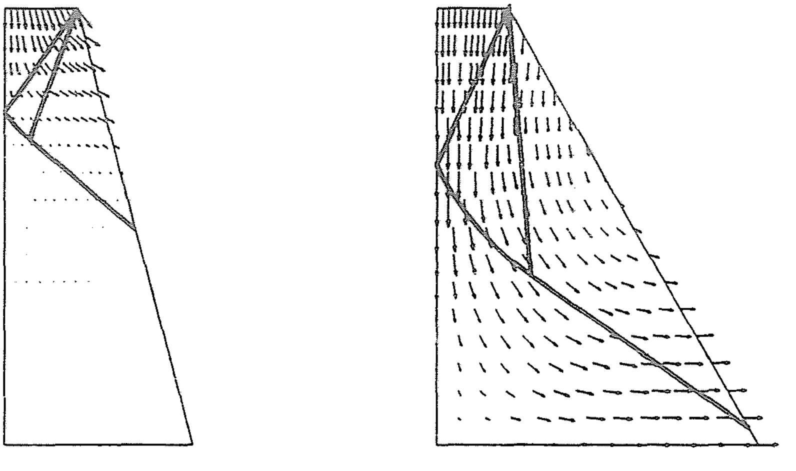

Fig. 6. Displacement in the last load step

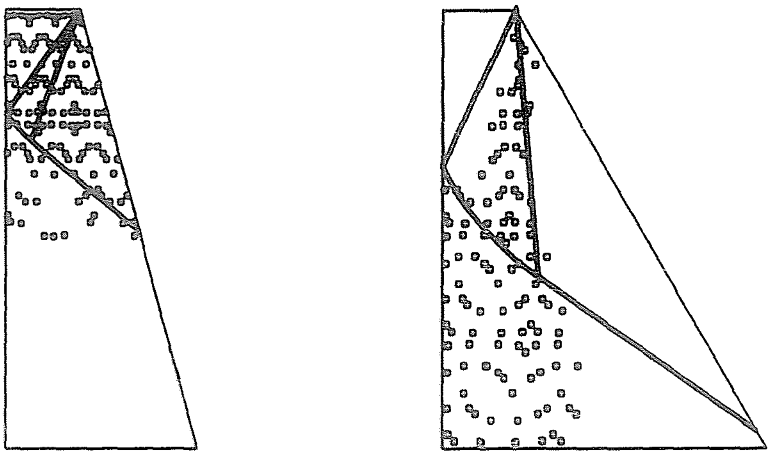

Fig. 7. Points of plasticity

In *Fig. 5*, the deformed shape of the finite element network is seen against the original shape shown in *Fig. 4*. Both here, and in the subsequent figures, gliding surfaces according to Jáky are also shown. Apparently, in the first case (steep side small angle of friction) displacements agree, with analytic results, but for less inclined sides and/or higher frictional angles the cutter side will have just an opposite displacement. In the case seen in the figure, there is just place for the development of analytically determinable sliding surface, but even so, the lower rim apparently has an important disturbing effect.

Vectors of displacements in the last loading step (after development of the failure mechanism) are seen in *Fig. 6*. Conclusions are similar to those from the former diagram. For the left-hand model, displacements are concentrated near the loaded surface and remain inside the analytically obtainable sliding surface. In the second model there are displacements almost in the entire model and the developing failure mechanism is quite different from that in the first model. Extension of the plastic zone is seen in *Fig. 7*. Marked points indicate those integration basic points of finite element networks (those of numerical integration needed for FEM) where the Mohr–Coulomb failure condition is fulfilled. In the first model the numerically obtained failure mechanism is similar to that obtained analytically. The second model is entirely different, in that here the plastic zone develops below a wedge pressing in at the middle, shifting laterally the remaining also wedge shaped parts and producing displacements seen in *Fig. 6*. Application of the Mohr–Coulomb failure condition for concrete footings.

The Mohr–Coulomb model generally valid for soils also suits investigation of concrete structures. From strength characteristics of concrete (compressive and tensile strength) two characteristics of the applied soil model: cohesion, and internal friction angle, may be determined (SZALAI, 1988).

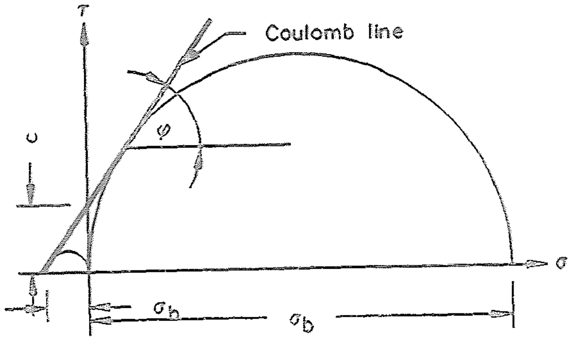

Fig. 8. Mohr–Coulomb model of concrete

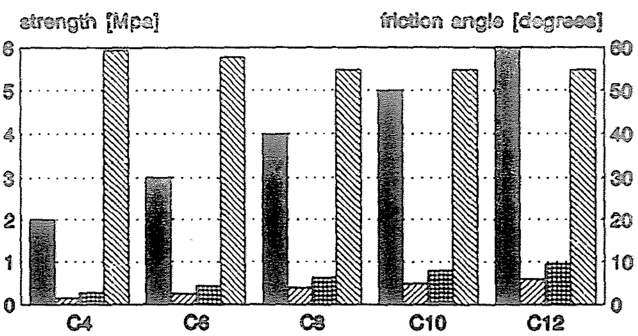

	C4	C6	C8	C10	C12
sigma b	2	3	4	5	6
sigma h	0.15	0.25	0.4	0.5	0.6
c	0.274	0.433	0.632	0.79	0.949
phi	59.4	57.8	54.9	54.9	54.9

Fig. 9. Concrete shear strength values

According to *Fig. 8*:

$$C = \frac{1}{2}\sqrt{\sigma_b \sigma_h} \tag{5}$$

$$\varphi = 90^\circ - 2\arctan\sqrt{\frac{\sigma_h}{\sigma_b}} \tag{6}$$

Compressive and shear strength values for various quality categories of concrete are seen in *Fig. 9*.

Further Problems

As was discussed in the preceding, results obtained analytically by Jáky and Kézdi are unsuitable for designing footings because of their shapes and the high internal friction angle of concrete. Design for pure bending is even less justified. It seems advisable to compile a table of diagram by FEM analysis to aid design. After Jáky and Kézdi, the investigation may be extended — for strip foundations — to inclined loading. The PLAXIS program also suits problems of axial symmetry, so it may be applied for designing square pier footings under vertical loads, at a fair approximation. For analytically checking the outputs — if needed — modified failure mechanism according to *Fig. 7* has to be applied. Also the effect of expansion typical of materials of large angles of friction has to be examined.

References

JÁKY, J. (1945): Composite Compressive Stress States. I. Cutting, Piercing and Splitting Resistances (in Hungarian). *Technika*, No. 246, Budapest.

KÉZDI, Á. (1970): Soil Mechanics II. (in Hungarian). Tankönyvkiadó, Budapest.

SZALAI, K. (1988): Reinforced Concrete Structures (in Hungarian). Tankönyvkiadó, Budapest.

VERMEER, P. A. (ed., 1993): PLAXIS, Finite Element Code for Soil and Rock Plasticity. A. A. Balkema, Rotterdam, Brookfield.